Superconductivity in Cu-doped Bi_2Se_3 with potential disorder

Takumi Sato [1] and Yasuhiro Asano [1,2]
[1] *Department of Applied Physics, Hokkaido University, Sapporo 060-8628, Japan*
[2] *Center of Topological Science & Technology, Hokkaido University, Sapporo 060-8628, Japan*

(Received 21 April 2020; revised 1 July 2020; accepted 7 July 2020; published 17 July 2020)

We study the effects of random nonmagnetic impurities on superconducting transition temperature T_c in a Cu-doped Bi_2Se_3, for which four types of pair potentials have been proposed. Although all the candidates belong to s-wave symmetry, two orbital degrees of freedom in electronic structures enrich the symmetry variety of a Cooper pair such as even-orbital-parity and odd-orbital-parity. We consider realistic electronic structures of Cu-doped Bi_2Se_3 by using a tight-binding Hamiltonian on a hexagonal lattice and consider effects of impurity scatterings through the self-energy of the Green's function within the Born approximation. We find that even-orbital-parity spin-singlet superconductivity is basically robust even in the presence of impurities. The degree of the robustness depends on the electronic structures in the normal state and on the pairing symmetry in orbital space. On the other hand, two odd-orbital-parity spin-triplet order parameters are always fragile in the presence of potential disorder.

DOI: 10.1103/PhysRevB.102.024516

I. INTRODUCTION

The robustness of superconductivity in the presence of nonmagnetic impurities depends on symmetry of the pair potential. The transition temperature T_c is insensitive to the impurity concentration in a spin-singlet s-wave superconductor [1–3]. In a cuprate superconductor, on the other hand, T_c of a spin-singlet d-wave superconductivity is suppressed drastically by the impurity scatterings [4]. The pair potential of an unconventional superconductor changes its sign on the Fermi surface depending on the direction of a quasiparticle's momenta. The random impurity scatterings make the motion of a quasiparticle isotropic in both real and momentum spaces. Such a diffused quasiparticle feels the pair potential averaged over the directions of momenta. The resulting pair potential is finite for an s-wave symmetry, whereas it is zero for unconventional pairing symmetries. Thus, unconventional superconductivity is fragile under the potential disorder.

Previous papers [5–10] showed that s-wave superconductivity is not always robust against the nonmagnetic impurity scatterings in multiband (multiorbital) superconductors. The interorbital impurity scatterings decrease T_c, which is a common conclusion of theoretical studies. The two-band models considered in these papers, however, are too simple to discuss the effects of impurities on T_c in real materials such as iron pnictides [11,12], MgB_2 [13,14], and Cu-doped Bi_2Se_3 [15,16]. The robustness of multiband superconductivity under the potential disorder may depend on electronic structures near the Fermi level. In iron pnictides and MgB_2, two electrons in the same conduction band form a Cooper pair [12,14]. The impurity effect on such an intraband pair has been studied by taking realistic electronic structures into account [17]. In the case of Cu-doped Bi_2Se_3, four types of pair potentials $\Delta_1 - \Delta_4$ have been proposed as a promising candidate of order parameters [16]. Among them, an interorbital pairing order has attracted much attention as a topologically nontrivial superconductivity [16,18]. Unfortunately, the possibility of such a topological superconductivity under the potential disorder hasn't been studied yet. We address this issue.

In this paper, we study the effects of impurities on T_c of Cu-doped Bi_2Se_3. We describe electronic structures near the Fermi level by taking into account two p orbitals in Bi_2Se_3 and the hybridization between them [19,20]. According to the theoretical proposal [16], we consider four types of s-wave pair potentials on such orbital-based electronic structures. The effects of impurities on T_c are estimated through the impurity self-energy within the Born approximation. The transition temperature is calculated by solving the gap equation numerically and is plotted as a function of impurity concentration $n_{\rm imp}$. We will show that the relation between T_c and $n_{\rm imp}$ depends sensitively on the types of pair potentials. Superconductivity with an intraorbital pair potential Δ_1 is robust even in the dirty regime. This conclusion is consistent with that at a limiting case of previous studies [6–9]. There are two kinds of interorbital pairing order: even-orbital symmetry and odd-orbital symmetry. We find that T_c of an even-interorbital superconductivity Δ_3 decreases slowly with the increase of $n_{\rm imp}$ and vanishes in the dirty limit. The results for Δ_3 disagree with those in a simple two-band model [10] because the robustness of Δ_3 depends sensitively on electronic structures. Finally, the odd-interorbital pairing orders (Δ_2 and Δ_4) vanish at a critical value of the impurity concentration, which agrees well with the results of an idealistic two-band model [10]. Thus we conclude that odd-orbital pair potential is fragile irrespective of electronic structures.

This paper is organized as follows. In Sec. II, we describe the effective Hamiltonian near the Fermi level in Cu-doped Bi_2Se_3 and four types of pair potentials in its superconducting state. The anomalous Green's function and the gap equation for each pair potential in the clean limit are obtained by solving the Gor'kov equation. In Sec. III, we introduce the random impurity potential and discuss the effects of impurities on T_c within the Born approximation. The conclusion is given in Sec. IV. Throughout this paper, we use units of $k_{\rm B} = \hbar = 1$,

 ©2020 American Physical Society

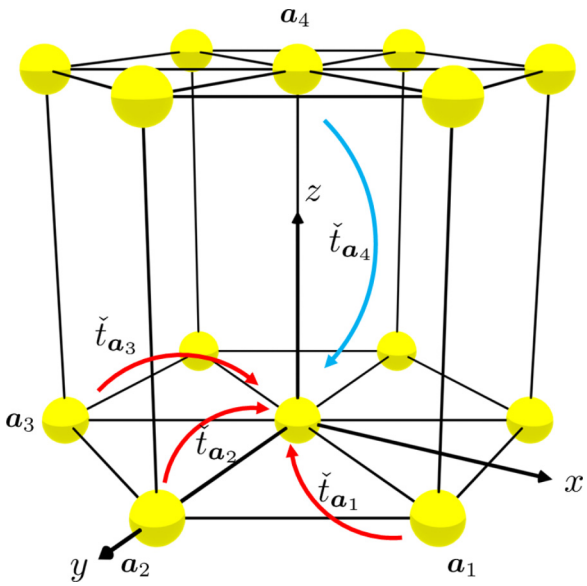

FIG. 1. The simplified lattice structure of a Cu-doped Bi_2Se_3. The arrow indicates the hopping.

where k_B is the Boltzmann constant. The symbols $\cdot\bar{\cdot}\cdot$, $\cdot\check{\cdot}\cdot$, and $\cdot\hat{\cdot}\cdot$ represent 8×8, 4×4, and 2×2 matrices, respectively.

II. CLEAN LIMIT

A. Model

For constructing an effective model of the normal state, we start with the tight-binding Hamiltonian on a hexagonal lattice as shown in Fig. 1 [21]. Strictly speaking, the crystal structure of Bi_2Se_3 is rhombohedral [19,20]. The simplification does not affect the low-energy physics. We assume that an intercalated copper atom supplies electrons and makes topological insulator Bi_2Se_3 be metallic [22]. In the hexagonal lattice, the primitive lattice vectors are $(\sqrt{3}a/2, a/2, 0)$, $(0, a, 0)$, $(0, 0, c)$, where a and c are the lattice constants in the xy plane and along the z axis, respectively. We define the nearest-neighbor vectors $\boldsymbol{a}_1 = (\sqrt{3}a/2, a/2, 0)$, $\boldsymbol{a}_2 = (0, a, 0)$, $\boldsymbol{a}_3 = (-\sqrt{3}a/2, a/2, 0)$, and $\boldsymbol{a}_4 = (0, 0, c)$. The tight-binding Hamiltonian in real space can be written as [21,23]

$$H_N = \sum_{\boldsymbol{R}} \boldsymbol{\psi}_{\boldsymbol{R}}^{\dagger} \check{\varepsilon} \boldsymbol{\psi}_{\boldsymbol{R}} + \sum_{\boldsymbol{R},i} \boldsymbol{\psi}_{\boldsymbol{R}}^{\dagger} \check{t}_{\boldsymbol{a}_i} \boldsymbol{\psi}_{\boldsymbol{R}+\boldsymbol{a}_i} + \text{H.c.}, \tag{1}$$

$$\boldsymbol{\psi}_{\boldsymbol{R}} = [\psi_{+,\uparrow}(\boldsymbol{R}),\ \psi_{-,\uparrow}(\boldsymbol{R}),\ \psi_{+,\downarrow}(\boldsymbol{R}),\ \psi_{-,\downarrow}(\boldsymbol{R})]^{\mathrm{T}}, \tag{2}$$

where $\psi_{\sigma,s}^{\dagger}$ ($\psi_{\sigma,s}$) is the creation (annihilation) operator of an electron at the orbital σ ($=+$ or $-$) with spin s ($=\uparrow$ or $\downarrow$). We consider only the nearest-neighbor hopping on the hexagonal lattice in the xy plane and that along the z axis. An orbital $+$ ($-$) mainly consists of p_z orbital of a Bi (Se) atom. The matrix element of hopping $\check{t}_{\boldsymbol{a}_i}$ ($i = 1-4$) is described as

$$\langle \boldsymbol{R}, \sigma, s | H | \boldsymbol{R}+\boldsymbol{a}_i, \sigma', s' \rangle . \tag{3}$$

The nearest-neighbor hopping elements are illustrated in Fig. 1. In momentum space, the tight-binding Hamiltonian is described as

$$\check{H}_N(\boldsymbol{k}) = \check{\varepsilon} + \sum_i \check{t}_{\boldsymbol{a}_i} e^{i\boldsymbol{k}\cdot\boldsymbol{a}_i} + \text{H.c.} \tag{4}$$

The matrix structures of $\check{t}_{\boldsymbol{a}_i}$ are given in Appendix A. The tight-binding Hamiltonian can be written as

$$\check{H}_N(\boldsymbol{k}) = c_{\boldsymbol{k}}\hat{s}_0\hat{\sigma}_0 + m_{\boldsymbol{k}}\hat{s}_0\hat{\sigma}_3 + V_z\hat{s}_0\hat{\sigma}_2 + (V_y\hat{s}_1 - V_x\hat{s}_2)\hat{\sigma}_1, \tag{5}$$

$$c_{\boldsymbol{k}} = -\mu + c_1\alpha_1(\boldsymbol{k}) + c_2\alpha_2(\boldsymbol{k}), \tag{6}$$

$$m_{\boldsymbol{k}} = m_0 + m_1\alpha_1(\boldsymbol{k}) + m_2\alpha_2(\boldsymbol{k}), \tag{7}$$

$$V_{x,y} = v\alpha_{x,y}(\boldsymbol{k}), \tag{8}$$

$$V_z = v_z\alpha_z(\boldsymbol{k}), \tag{9}$$

where $\alpha_i(\boldsymbol{k})$ ($i = 1, 2, x, y, z$) is

$$\alpha_1(\boldsymbol{k}) = \frac{2}{c^2}(1 - \cos k_z c), \tag{10}$$

$$\alpha_2(\boldsymbol{k}) = \frac{4}{3a^2}\left(3 - 2\cos\frac{\sqrt{3}k_x a}{2}\cos\frac{k_y a}{2} - \cos k_y a\right), \tag{11}$$

$$\alpha_x(\boldsymbol{k}) = \frac{2}{\sqrt{3}a}\sin\frac{\sqrt{3}k_x a}{2}\cos\frac{k_y a}{2}, \tag{12}$$

$$\alpha_y(\boldsymbol{k}) = \frac{2}{3a}\left(\cos\frac{\sqrt{3}k_x a}{2}\sin\frac{k_y a}{2} + \sin k_y a\right), \tag{13}$$

$$\alpha_z(\boldsymbol{k}) = \frac{1}{c}\sin k_z c. \tag{14}$$

We define Pauli matrices $\hat{s}_j$ in spin space, $\hat{\sigma}_j$ in orbital space, and $\hat{\tau}_j$ in particle-hole space for $j = 1-3$. The unit matrix in these spaces are $\hat{s}_0$, $\hat{\sigma}_0$, and $\hat{\tau}_0$. In Eq. (5), the hopping in the z direction ($\check{t}_{\boldsymbol{a}_4}$) causes the orbital hybridization term V_z and the hopping in the xy plane ($\check{t}_{\boldsymbol{a}_1}$, $\check{t}_{\boldsymbol{a}_2}$, $\check{t}_{\boldsymbol{a}_3}$) causes the spin-orbit interaction term $V_{x,y}$. When we expand the trigonometric functions around the Γ point, the tight-binding Hamiltonian $\check{H}_N(\boldsymbol{k})$ corresponds to $\boldsymbol{k}\cdot\boldsymbol{p}$ Hamiltonian of Bi_2Se_3 [19,20].

The superconducting state in $Cu_xBi_2Se_3$ is described by a Hamiltonian

$$\mathcal{H}^{(0)} = \sum_{\boldsymbol{k}} \boldsymbol{\Psi}^{\dagger}(\boldsymbol{k})\bar{H}_{\boldsymbol{k}}^{(0)}\boldsymbol{\Psi}(\boldsymbol{k}), \quad \boldsymbol{\Psi}(\boldsymbol{k}) = \begin{bmatrix} \boldsymbol{\psi}_e(\boldsymbol{k}) \\ \boldsymbol{\psi}_h(\boldsymbol{k}) \end{bmatrix}, \tag{15}$$

$$\boldsymbol{\psi}_e(\boldsymbol{k}) = \begin{bmatrix} \psi_{+,\uparrow}(\boldsymbol{k}) \\ \psi_{-,\uparrow}(\boldsymbol{k}) \\ \psi_{+,\downarrow}(\boldsymbol{k}) \\ \psi_{-,\downarrow}(\boldsymbol{k}) \end{bmatrix}, \quad \boldsymbol{\psi}_h(\boldsymbol{k}) = \begin{bmatrix} \psi_{+,\uparrow}^{\dagger}(-\boldsymbol{k}) \\ \psi_{-,\uparrow}^{\dagger}(-\boldsymbol{k}) \\ \psi_{+,\downarrow}^{\dagger}(-\boldsymbol{k}) \\ \psi_{-,\downarrow}^{\dagger}(-\boldsymbol{k}) \end{bmatrix}, \tag{16}$$

$$\bar{H}_{\boldsymbol{k}}^{(0)} = \begin{pmatrix} \check{H}_N(\boldsymbol{k}) & \check{\Delta}_\lambda \\ \check{\Delta}_\lambda^{\dagger} & -\check{H}_N^{*}(-\boldsymbol{k}) \end{pmatrix}. \tag{17}$$

According to the previous proposal [16], we consider four types of momentum-independent pair potential defined by

$$\Delta_1 = \frac{g_1}{N}\sum_{\boldsymbol{k}} \langle \psi_{+,\uparrow}(\boldsymbol{k})\psi_{+,\downarrow}(-\boldsymbol{k})\rangle = \frac{g_1}{N}\sum_{\boldsymbol{k}} \langle \psi_{-,\uparrow}(\boldsymbol{k})\psi_{-,\downarrow}(-\boldsymbol{k})\rangle, \tag{18}$$

$$\Delta_2 = \frac{g_2}{N}\sum_{\boldsymbol{k}}\langle\psi_{+,\uparrow}(\boldsymbol{k})\psi_{-,\downarrow}(-\boldsymbol{k})\rangle = -\frac{g_2}{N}\sum_{\boldsymbol{k}}\langle\psi_{-,\uparrow}(\boldsymbol{k})\psi_{+,\downarrow}(-\boldsymbol{k})\rangle, \tag{19}$$

$$\Delta_3 = \frac{g_3}{N}\sum_{\boldsymbol{k}}\langle\psi_{+,\uparrow}(\boldsymbol{k})\psi_{-,\downarrow}(-\boldsymbol{k})\rangle = \frac{g_3}{N}\sum_{\boldsymbol{k}}\langle\psi_{-,\uparrow}(\boldsymbol{k})\psi_{+,\downarrow}(-\boldsymbol{k})\rangle, \tag{20}$$

$$\Delta_4 = \frac{g_4}{N}\sum_{\boldsymbol{k}}\langle\psi_{+,\uparrow}(\boldsymbol{k})\psi_{-,\uparrow}(-\boldsymbol{k})\rangle = -\frac{g_4}{N}\sum_{\boldsymbol{k}}\langle\psi_{-,\uparrow}(\boldsymbol{k})\psi_{+,\uparrow}(-\boldsymbol{k})\rangle, \tag{21}$$

where $g_\lambda > 0$ ($\lambda = 1-4$) represents the attractive interaction between two electrons. Generally speaking, the pair correlation function can be represented as

$$f_{s,\sigma;s',\sigma'}(\boldsymbol{k}) = \langle\psi_{s,\sigma}(\boldsymbol{k})\,\psi_{s',\sigma'}(-\boldsymbol{k})\rangle, \tag{22}$$

where we assume a spatially uniform equal-time Cooper pair. The momentum-symmetry is even-parity s-wave symmetry, which is a common property among the four candidates in a Cu-doped Bi_2Se_3. Because of the Fermi-Dirac statistics of electrons, the pairing correlation obeys

$$f_{s,\sigma;s',\sigma'}(\boldsymbol{k}) = -f_{s',\sigma';s,\sigma}(\boldsymbol{k}). \tag{23}$$

The remaining symmetry options of the pairing function are orbitals and spins of a Cooper pair. Therefore, the pairing function must be either antisymmetric under $s \leftrightarrow s'$ or antisymmetric under $\sigma \leftrightarrow \sigma'$.

Both Eqs. (18) and (20) belong to spin-singlet symmetry. Thus the pairing functions belong to even-orbital parity. In Eq. (20), a Cooper pair consists of two electrons in the different orbitals (interorbital pair): one electron is in + orbital and the other is in − orbital. In Eq. (18), on the other hand, a Cooper pair consists of two electrons in the same orbital (intraorbital pair). The pair potential in the + orbital and that in the − orbital have the same amplitude and the same sign.

Both Eqs. (19) and (21) represent the spin-triplet interorbital pairing correlations. In these cases, the pair correlation belongs to odd-orbital-parity symmetry. In addition to the symmetry options for Cooper pairing, the pair potentials are classified by the irreducible representation of D_{3d} point group. Δ_2 and Δ_4 can be distinguished from each other by the irreducible representation. The matrix form of pair potentials, the irreducible representation, spin symmetry, and orbital-parity of the pair potentials are summarized in Table I. Although Fu and Berg [16] proposed a pair potential of $\Delta(i\hat{s}_2)\hat{\sigma}_3$, it is unitary equivalent to Eq. (18) as long as the Hamiltonian $\bar{H}^{(0)}_{\boldsymbol{k}}$ preserves time-reversal symmetry [9]. (See Appendix B for details.) They also considered a pair potential of $\Delta\hat{s}_0(i\hat{\sigma}_2)$ independently of Eq. (21). However, the behavior of T_c under the potential disorder in the two pair potentials are the same as each other. Thus, in this paper, we discuss effects of random impurity scatterings on superconducting states described by Eqs. (18)–(21). We note that the orbital parity and the momentum parity are independent symmetry options of each other. The former represents symmetry of correlation functions under the commutation of two orbitals. The latter is derived from inversion symmetry of the lattice structure.

TABLE I. Symmetry classification of pair potentials. Equal-time pairing order parameter belongs to even-frequency symmetry. A spin-singlet component is described by $i\hat{s}_2$. An opposite-spin-triplet and an equal-spin-triplet components are indicated by $\hat{s}_1$ and $\hat{s}_3$, respectively.

Matrix	Rep.	Frequency	Spin	Momentum parity	Orbital parity
$\Delta_1(i\hat{s}_2)\hat{\sigma}_0$	A_{1g}	Even	Singlet	Even	Even (Intra)
$\Delta_2\hat{s}_1(i\hat{\sigma}_2)$	A_{1u}	Even	Triplet	Even	Odd (Inter)
$\Delta_3(i\hat{s}_2)\hat{\sigma}_1$	A_{2u}	Even	Singlet	Even	Even (Inter)
$\Delta_4\hat{s}_3(i\hat{\sigma}_2)$	E_u	Even	Triplet	Even	Odd (Inter)

In addition to the pair potentials in Eqs. (18)–(21), generally speaking, the mean-field Hamiltonian contains the interorbital Cooper pair scattering terms described as

$$g'_\lambda\langle\psi^\dagger_{\sigma',s'}(-\boldsymbol{k}')\psi^\dagger_{\gamma',s}(\boldsymbol{k}')\rangle\psi_{\gamma,s}(\boldsymbol{k})\psi_{\sigma,s'}(-\boldsymbol{k}), \tag{24}$$

with $\gamma \neq \gamma'$ and $\sigma \neq \sigma'$ [24]. We do not consider these terms because they only renormalize the amplitude of the pair potential as

$$\Delta_\lambda \to \Delta_\lambda\left(1 + P\frac{g'_\lambda}{g_\lambda}\right), \tag{25}$$

and do not change main conclusions of this paper, where P is 1 (−1) for the even- (odd-) orbital-parity superconductivity.

B. Gor'kov equation

The Matsubara Green's function is obtained by solving the Gor'kov equation,

$$[i\omega_n - \check{H}^{(0)}(\boldsymbol{k})]\bar{G}^{(0)}(\boldsymbol{k}, i\omega_n) = 1, \tag{26}$$

$$\bar{G}^{(0)}(\boldsymbol{k}, i\omega_n) = \begin{pmatrix} \check{\mathcal{G}}^{(0)}(\boldsymbol{k}, i\omega_n) & \check{\mathcal{F}}^{(0)}_\lambda(\boldsymbol{k}, i\omega_n) \\ -\check{\mathcal{F}}^{(0)*}_\lambda(-\boldsymbol{k}, i\omega_n) & -\check{\mathcal{G}}^{(0)*}(-\boldsymbol{k}, i\omega_n) \end{pmatrix}, \tag{27}$$

where $\omega_n = (2n+1)\pi T$ is a fermionic Matsubara frequency and T is a temperature. To discuss the transition temperature, we need to find the solutions of Eq. (26) within the first order of Δ. The results of the normal part

$$\check{\mathcal{G}}^{(0)}(\boldsymbol{k}, i\omega_n) = \frac{1}{X}[(i\omega_n - c_{\boldsymbol{k}})\,\hat{s}_0\hat{\sigma}_0 + m_{\boldsymbol{k}}\,\hat{s}_0\hat{\sigma}_3 + V_z\,\hat{s}_0\hat{\sigma}_2 + (V_y\hat{s}_1 - V_x\hat{s}_2)\,\hat{\sigma}_1], \tag{28}$$

$$X(\boldsymbol{k}, i\omega_n) = (i\omega_n - c_{\boldsymbol{k}})^2 - m^2_{\boldsymbol{k}} - V_x^2 - V_y^2 - V_z^2, \tag{29}$$

are common for all the pair potentials because the normal Green's function does not include the pair potential at the lowest order. The results of the anomalous Green's function

are given by

$$\check{\mathcal{F}}_1^{(0)}(\boldsymbol{k}, i\omega_n) = \frac{\Delta_1}{Z}\big[-i\big(\omega_n^2 + c_{\boldsymbol{k}}^2 + m_{\boldsymbol{k}}^2 + V_x^2 + V_y^2 + V_z^2\big)\,\hat{s}_2\hat{\sigma}_0 + 2ic_{\boldsymbol{k}}m_{\boldsymbol{k}}\,\hat{s}_2\hat{\sigma}_3 + 2ic_{\boldsymbol{k}}V_z\,\hat{s}_2\hat{\sigma}_2 - 2c_{\boldsymbol{k}}V_y\,\hat{s}_3\hat{\sigma}_1 - 2ic_{\boldsymbol{k}}V_x\,\hat{s}_0\hat{\sigma}_1\big], \tag{30}$$

$$\check{\mathcal{F}}_2^{(0)}(\boldsymbol{k}, i\omega_n) = \frac{\Delta_2}{Z}\big[-i\big(\omega_n^2 + c_{\boldsymbol{k}}^2 - m_{\boldsymbol{k}}^2 + V_x^2 + V_y^2 + V_z^2\big)\,\hat{s}_1\hat{\sigma}_2 + 2m_{\boldsymbol{k}}V_y\,\hat{s}_0\hat{\sigma}_0 - 2c_{\boldsymbol{k}}V_y\,\hat{s}_0\hat{\sigma}_3 + 2im_{\boldsymbol{k}}V_x\,\hat{s}_3\hat{\sigma}_0 - 2ic_{\boldsymbol{k}}V_x\,\hat{s}_3\hat{\sigma}_3$
$+ 2ic_{\boldsymbol{k}}V_z\,\hat{s}_1\hat{\sigma}_0 - 2im_{\boldsymbol{k}}V_z\,\hat{s}_1\hat{\sigma}_3 + 2i\omega_n m_{\boldsymbol{k}}\,\hat{s}_1\hat{\sigma}_1\big], \tag{31}$$

$$\check{\mathcal{F}}_3^{(0)}(\boldsymbol{k}, i\omega_n) = \frac{\Delta_3}{Z}\big[-i\big(\omega_n^2 + c_{\boldsymbol{k}}^2 - m_{\boldsymbol{k}}^2 + V_x^2 + V_y^2 - V_z^2\big)\big)\,\hat{s}_2\hat{\sigma}_1 + 2iV_xV_z\,\hat{s}_0\hat{\sigma}_2 + 2V_yV_z\,\hat{s}_3\hat{\sigma}_2 - 2ic_{\boldsymbol{k}}V_x\,\hat{s}_0\hat{\sigma}_0 + 2im_{\boldsymbol{k}}V_x\,\hat{s}_0\hat{\sigma}_3$
$-2c_{\boldsymbol{k}}V_y\,\hat{s}_3\hat{\sigma}_0 + 2m_{\boldsymbol{k}}V_y\,\hat{s}_3\hat{\sigma}_3 - 2i\omega_n m_{\boldsymbol{k}}\,\hat{s}_2\hat{\sigma}_2 + 2i\omega_n V_z\,\hat{s}_2\hat{\sigma}_3\big], \tag{32}$$

$$\check{\mathcal{F}}_4^{(0)}(\boldsymbol{k}, i\omega_n) = \frac{\Delta_4}{Z}\big[-i\big(\omega_n^2 + c_{\boldsymbol{k}}^2 - m_{\boldsymbol{k}}^2 + V_x^2 - V_y^2 + V_z^2\big)\,\hat{s}_3\hat{\sigma}_2 - 2V_xV_y\,\hat{s}_0\hat{\sigma}_2 - 2im_{\boldsymbol{k}}\,V_x\hat{s}_1\hat{\sigma}_0 + 2ic_{\boldsymbol{k}}V_x\,\hat{s}_1\hat{\sigma}_3 + 2ic_{\boldsymbol{k}}V_z\,\hat{s}_3\hat{\sigma}_0$
$-2im_{\boldsymbol{k}}V_z\,\hat{s}_3\hat{\sigma}_3 - 2V_yV_z\,\hat{s}_2\hat{\sigma}_1 + 2i\omega_n m_{\boldsymbol{k}}\,\hat{s}_3\hat{\sigma}_1 - 2\omega_n V_y\,\hat{s}_2\hat{\sigma}_3\big], \tag{33}$$

with $Z(\boldsymbol{k}, i\omega_n) = |X(\boldsymbol{k}, i\omega_n)|^2$. The $\hat{s}_2\hat{\sigma}_0$ component in Eq. (30), the $\hat{s}_1\hat{\sigma}_2$ component in Eq. (31), the $\hat{s}_2\hat{\sigma}_1$ component in Eq. (32), and the $\hat{s}_3\hat{\sigma}_2$ component in Eq. (33) are linked to the pair potentials Δ_1, Δ_2, Δ_3, and Δ_4, respectively. Therefore, the gap equations in the linear regime result in

$$\Delta_1 = -g_1T\sum_{\omega_n}\frac{1}{N}\sum_{\boldsymbol{k}}\mathrm{Tr}\left[\check{\mathcal{F}}_1^{(0)}(\boldsymbol{k}, i\omega_n)\frac{(-i\hat{s}_2)\hat{\sigma}_0}{4}\right] = g_1T\sum_{\omega_n}\frac{1}{N}\sum_{\boldsymbol{k}}\frac{\Delta_1}{Z(\boldsymbol{k}, i\omega_n)}\big[\omega_n^2 + c_{\boldsymbol{k}}^2 + m_{\boldsymbol{k}}^2 + V_x^2 + V_y^2 + V_z^2\big], \tag{34}$$

$$\Delta_2 = -g_2T\sum_{\omega_n}\frac{1}{N}\sum_{\boldsymbol{k}}\mathrm{Tr}\left[\check{\mathcal{F}}_2^{(0)}(\boldsymbol{k}, i\omega_n)\frac{\hat{s}_1(-i\hat{\sigma}_2)}{4}\right] = g_2T\sum_{\omega_n}\frac{1}{N}\sum_{\boldsymbol{k}}\frac{\Delta_2}{Z(\boldsymbol{k}, i\omega_n)}\big[\omega_n^2 + c_{\boldsymbol{k}}^2 - m_{\boldsymbol{k}}^2 + V_x^2 + V_y^2 + V_z^2\big], \tag{35}$$

$$\Delta_3 = -g_3T\sum_{\omega_n}\frac{1}{N}\sum_{\boldsymbol{k}}\mathrm{Tr}\left[\check{\mathcal{F}}_3^{(0)}(\boldsymbol{k}, i\omega_n)\frac{(-i\hat{s}_2)\hat{\sigma}_1}{4}\right] = g_3T\sum_{\omega_n}\frac{1}{N}\sum_{\boldsymbol{k}}\frac{\Delta_3}{Z(\boldsymbol{k}, i\omega_n)}\big[\omega_n^2 + c_{\boldsymbol{k}}^2 - m_{\boldsymbol{k}}^2 + V_x^2 + V_y^2 - V_z^2\big], \tag{36}$$

$$\Delta_4 = -g_4T\sum_{\omega_n}\frac{1}{N}\sum_{\boldsymbol{k}}\mathrm{Tr}\left[\check{\mathcal{F}}_4^{(0)}(\boldsymbol{k}, i\omega_n)\frac{\hat{s}_3(-i\hat{\sigma}_2)}{4}\right] = g_4T\sum_{\omega_n}\frac{1}{N}\sum_{\boldsymbol{k}}\frac{\Delta_4}{Z(\boldsymbol{k}, i\omega_n)}\big[\omega_n^2 + c_{\boldsymbol{k}}^2 - m_{\boldsymbol{k}}^2 + V_x^2 - V_y^2 + V_z^2\big]. \tag{37}$$

Equations (30)–(33) show that the orbital hybridization (V_z), the spin-orbit interaction ($V_{x,y}$), and the asymmetry between the two orbitals ($m_{\boldsymbol{k}}$) generate various paring correlations which belong to different symmetry classes from that of the pair potential [25,26]. Especially, we discuss briefly a role of odd-frequency pairing correlation in the gap equation. For instance, the pairing correlation $\check{\mathcal{F}}_2^{(0)}$ includes $2i\omega_n m_{\boldsymbol{k}}\,\hat{s}_1\hat{\sigma}_1$ which describes a spin-triplet even-orbital-parity component. Such a component must be odd-frequency symmetry because the pairing correlation function must be antisymmetric under the permutation of two electrons. In the gap equation, the odd-frequency pairing component decreases the numerator as shown in $-m_{\boldsymbol{k}}^2$ in Eq. (35). It has been pointed out that an odd-frequency pair decreases the transition temperature [26]. If we would be able to tune the parameters to delete more of the odd-frequency components, the gap equation results in higher T_c.

III. EFFECTS OF DISORDER

We consider the random nonmagnetic impurities described by

$$\bar{H}_{\mathrm{imp}}(\boldsymbol{R}) = V_{\mathrm{imp}}(\boldsymbol{R})\,\hat{\tau}_3\hat{s}_0(\hat{\sigma}_0 + \hat{\sigma}_1). \tag{38}$$

The schematic picture of potential disorder in a $Cu_xBi_2Se_3$ is shown in Fig. 2. We assume the impurity potential satisfies the following properties:

$$\overline{V_{\mathrm{imp}}(\boldsymbol{R})} = 0, \tag{39}$$

$$\overline{V_{\mathrm{imp}}(\boldsymbol{R})V_{\mathrm{imp}}(\boldsymbol{R}')} = n_{\mathrm{imp}}v_{\mathrm{imp}}^2\delta_{\boldsymbol{R},\boldsymbol{R}'}, \tag{40}$$

where $\overline{\cdots}$ means the ensemble average, n_{imp} is the density of the impurities, and v_{imp} is the strength of the impurity potential. We also assume that the attractive interactions between two electrons are insensitive to the impurity potentials [3]. We calculate the Green's function in the presence of the impurity potentials within the Born approximation. The Green's function is expanded up to the second order of the impurity potential:

$$\bar{G}(\boldsymbol{R}-\boldsymbol{R}', \omega_n) \approx \bar{G}^{(0)}(\boldsymbol{R}-\boldsymbol{R}', \omega_n) + \sum_{\boldsymbol{R}_1}\bar{G}^{(0)}(\boldsymbol{R}-\boldsymbol{R}_1, \omega_n)\overline{\bar{H}_{\mathrm{imp}}(\boldsymbol{R}_1)}\bar{G}^{(0)}(\boldsymbol{R}_1-\boldsymbol{R}', \omega_n) + \sum_{\boldsymbol{R}_1,\boldsymbol{R}_2}\bar{G}^{(0)}(\boldsymbol{R}-\boldsymbol{R}_1, \omega_n)$
$\times\overline{\bar{H}_{\mathrm{imp}}(\boldsymbol{R}_1)\bar{G}^{(0)}(\boldsymbol{R}_1-\boldsymbol{R}_2, \omega_n)\bar{H}_{\mathrm{imp}}(\boldsymbol{R}_2)}\bar{G}(\boldsymbol{R}_2-\boldsymbol{R}', \omega_n), \tag{41}$$

$$\approx \bar{G}^{(0)}(\boldsymbol{R}-\boldsymbol{R}',\omega_n) + n_{\rm imp} v_{\rm imp}^2 \sum_{\boldsymbol{R}_1} \bar{G}^{(0)}(\boldsymbol{R}-\boldsymbol{R}_1,\omega_n)\,\hat{\tau}_3\,\hat{s}_0\,\hat{\sigma}_0 \bar{G}^{(0)}(0,\omega_n)\,\hat{\tau}_3\,\hat{s}_0\,\hat{\sigma}_0 \bar{G}(\boldsymbol{R}_1-\boldsymbol{R}',\omega_n)$$
$$+ n_{\rm imp} v_{\rm imp}^2 \sum_{\boldsymbol{R}_1} \bar{G}^{(0)}(\boldsymbol{R}-\boldsymbol{R}_1,\omega_n)\,\hat{\tau}_3\,\hat{s}_0\,\hat{\sigma}_1 \bar{G}^{(0)}(0,\omega_n)\,\hat{\tau}_3\,\hat{s}_0\,\hat{\sigma}_1 \bar{G}(\boldsymbol{R}_1-\boldsymbol{R}',\omega_n). \tag{42}$$

We transform Eq. (41) to (42) by using the properties in Eqs. (39) and (40). In momentum space, Eq. (42) becomes

$$\bar{G}(\boldsymbol{k},i\omega_n) = \bar{G}^{(0)}(\boldsymbol{k},i\omega_n) + \bar{G}^{(0)}(\boldsymbol{k},i\omega_n)\bar{\Sigma}_{\rm imp}\bar{G}(\boldsymbol{k},i\omega_n), \tag{43}$$

$$\bar{\Sigma}_{\rm imp} = \bar{\Sigma}_{\rm intra} + \bar{\Sigma}_{\rm inter}, \tag{44}$$

$$\bar{\Sigma}_{\rm intra} = n_{\rm imp} v_{\rm imp}^2 \hat{\tau}_3\hat{s}_0\hat{\sigma}_0 \frac{1}{N}\sum_{\boldsymbol{k}} \bar{G}^{(0)}(\boldsymbol{k},i\omega_n)\hat{\tau}_3\hat{s}_0\hat{\sigma}_0, \tag{45}$$

$$\bar{\Sigma}_{\rm inter} = n_{\rm imp} v_{\rm imp}^2 \hat{\tau}_3\hat{s}_0\hat{\sigma}_1 \frac{1}{N}\sum_{\boldsymbol{k}} \bar{G}^{(0)}(\boldsymbol{k},i\omega_n)\hat{\tau}_3\hat{s}_0\hat{\sigma}_1, \tag{46}$$

where $\bar{\Sigma}_{\rm intra}$ and $\bar{\Sigma}_{\rm inter}$ are the self-energy due to the intraorbital impurity scatterings and that of the interorbital impurity scatterings, respectively. We describe the total self-energy as follows:

$$\bar{\Sigma}_{\rm imp} = \bar{\Sigma}_{\rm intra} + \bar{\Sigma}_{\rm inter} = \begin{bmatrix} \check{\Sigma}_g & \check{\Sigma}_{f_\lambda} \\ -\check{\Sigma}^*_{f_\lambda} & -\check{\Sigma}^*_g \end{bmatrix}, \tag{47}$$

$$\check{\Sigma}_g = n_{\rm imp} v_{\rm imp}^2 [\check{g}^{(0)} + \hat{s}_0\hat{\sigma}_1\check{g}^{(0)}\hat{s}_0\hat{\sigma}_1], \tag{48}$$

$$\check{\Sigma}_{f_\lambda} = -n_{\rm imp} v_{\rm imp}^2 \big[\check{f}^{(0)}_\lambda + \hat{s}_0\hat{\sigma}_1\check{f}^{(0)}_\lambda\hat{s}_0\hat{\sigma}_1\big], \tag{49}$$

where we denote the momentum summation of the Green's function as $1/N\sum_{\boldsymbol{k}}\check{\mathcal{G}}^{(0)}(\boldsymbol{k},i\omega_n) = \check{g}^{(0)}$ and $1/N\sum_{\boldsymbol{k}}\check{\mathcal{F}}^{(0)}(\boldsymbol{k},i\omega_n) = \check{f}^{(0)}$. Therefore, the Gor'kov equation in the presence of the impurity potential is described by

$$[i\omega_n - \bar{H}_0(\boldsymbol{k}) - \bar{\Sigma}_{\rm imp}]\bar{G}(\boldsymbol{k},i\omega_n) = 1, \tag{50}$$

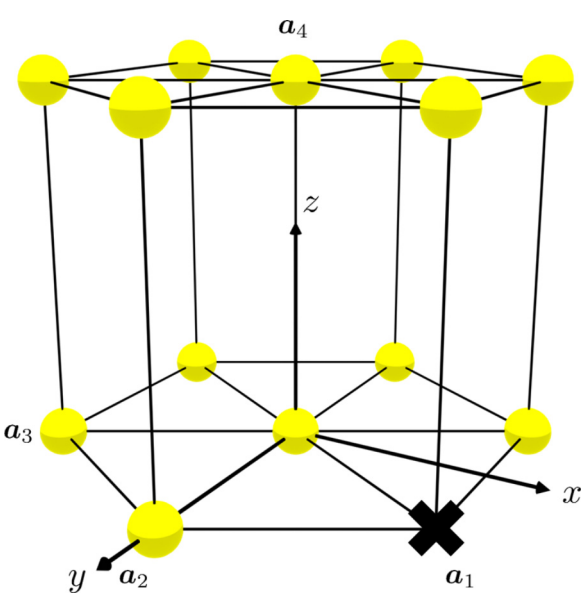

FIG. 2. A model of the random potential in a $Cu_xBi_2Se_3$. The cross mark denotes an impurity.

$$\bar{G}(\boldsymbol{k},i\omega_n) = \begin{pmatrix} \check{\mathcal{G}}(\boldsymbol{k},i\omega_n) & \check{\mathcal{F}}_\lambda(\boldsymbol{k},i\omega_n) \\ -\check{\mathcal{F}}^*_\lambda(-\boldsymbol{k},i\omega_n) & -\check{\mathcal{G}}^*(-\boldsymbol{k},i\omega_n) \end{pmatrix}. \tag{51}$$

The normal part of self-energy ($\check{\Sigma}_g$) is calculated as follows:

$$\check{\Sigma}_g = [-i\omega_n\eta_n + I_n]\,\hat{s}_0\hat{\sigma}_0, \tag{52}$$

$$\eta_n = n_{\rm imp} v_{\rm imp}^2 \frac{1}{N}\sum_{\boldsymbol{k}} \frac{2}{Z}\big[\omega_n^2 + c_{\boldsymbol{k}}^2 + m_{\boldsymbol{k}}^2 + V_x^2 + V_y^2 + V_z^2\big], \tag{53}$$

$$I_n = n_{\rm imp} v_{\rm imp}^2 \frac{1}{N}\sum_{\boldsymbol{k}} \frac{-2c_{\boldsymbol{k}}}{Z}\big[\omega_n^2 + c_{\boldsymbol{k}}^2 - m_{\boldsymbol{k}}^2 - V_x^2 - V_y^2 - V_z^2\big]. \tag{54}$$

Within the first order of Δ, the normal Green's function becomes

$$\check{\mathcal{G}}(\boldsymbol{k},i\omega_n) = \check{\mathcal{G}}^{(0)}(\boldsymbol{k},i\tilde{\omega}_n)|_{\mu\to\tilde{\mu}}, \tag{55}$$

$$\tilde{\omega}_n = \omega_n(1+\eta_n), \tag{56}$$

$$\tilde{\mu} = \mu - I_n. \tag{57}$$

The imaginary (real) part of the self-energy renormalizes the Matsubara frequency (chemical potential). The anomalous Green's function after summing up the momenta is described as

$$\check{f}^{(0)}_1 = \frac{1}{N}\sum_{\boldsymbol{k}} \frac{\Delta_1}{Z}\big[-i\big(\omega_n^2 + c_{\boldsymbol{k}}^2 + m_{\boldsymbol{k}}^2 + V_x^2 + V_y^2 + V_z^2\big)\,\hat{s}_2\hat{\sigma}_0 + 2ic_{\boldsymbol{k}}m_{\boldsymbol{k}}\,\hat{s}_2\hat{\sigma}_3\big], \tag{58}$$

$$\check{f}^{(0)}_2 = \frac{1}{N}\sum_{\boldsymbol{k}} \frac{\Delta_2}{Z}\big[-i\big(\omega_n^2 + c_{\boldsymbol{k}}^2 - m_{\boldsymbol{k}}^2 + V_x^2 + V_y^2 + V_z^2\big)\,\hat{s}_1\hat{\sigma}_2 + 2i\omega_n m_{\boldsymbol{k}}\,\hat{s}_1\hat{\sigma}_1\big], \tag{59}$$

$$\check{f}^{(0)}_3 = \frac{1}{N}\sum_{\boldsymbol{k}} \frac{\Delta_3}{Z}\big[-i\big(\omega_n^2 + c_{\boldsymbol{k}}^2 - m_{\boldsymbol{k}}^2 + V_x^2 + V_y^2 - V_z^2\big)\,\hat{s}_2\hat{\sigma}_1 - 2i\omega_n m_{\boldsymbol{k}}\,\hat{s}_2\hat{\sigma}_2\big], \tag{60}$$

$$\check{f}^{(0)}_4 = \frac{1}{N}\sum_{\boldsymbol{k}} \frac{\Delta_4}{Z}\big[-i\big(\omega_n^2 + c_{\boldsymbol{k}}^2 - m_{\boldsymbol{k}}^2 + V_x^2 - V_y^2 + V_z^2\big)\,\hat{s}_3\hat{\sigma}_2 + 2i\omega_n m_{\boldsymbol{k}}\,\hat{s}_3\hat{\sigma}_1\big]. \tag{61}$$

By substituting these expressions into Eq. (49), we obtain the anomalous part of the self-energy for each pair potential:

$$\check{\Sigma}_{f_1} = \Delta_1(i\hat{s}_2)\hat{\sigma}_0\cdot\eta_n, \tag{62}$$

$$\check{\Sigma}_{f_2} = \Delta_2\hat{s}_1\hat{\sigma}_1\cdot(-i\omega_n)J_n, \tag{63}$$

$$\check{\Sigma}_{f_3} = \Delta_3(i\hat{s}_2)\hat{\sigma}_1\cdot\eta'_n, \tag{64}$$

$$\check{\Sigma}_{f_4} = \Delta_4 \hat{s}_3 \hat{\sigma}_1 \cdot (-i\omega_n) J_n, \tag{65}$$

$$\eta'_n = n_{\rm imp} v_{\rm imp}^2 \frac{1}{N} \sum_{\boldsymbol{k}} \frac{2}{Z} \left[\omega_n^2 + c_{\boldsymbol{k}}^2 - m_{\boldsymbol{k}}^2 + V_x^2 + V_y^2 - V_z^2\right], \tag{66}$$

$$J_n = n_{\rm imp} v_{\rm imp}^2 \frac{1}{N} \sum_{\boldsymbol{k}} \frac{4 m_{\boldsymbol{k}}}{Z}. \tag{67}$$

Before demonstrating T_c under the potential disorder, we briefly summarize a relation between the self-energy and the pair potential in the four cases. The results in Eq. (62) show that $\check{\Sigma}_{f_1}$ has the same matrix structure with the pair potential as shown in Table I. Namely, $\check{\Sigma}_{f_1}$ renormalizes the pair potential Δ_1 which belongs to even-frequency spin-singlet even-momentum-parity even-orbital-parity pairing symmetry. We will show that this fact explains the robustness of Δ_1 in the presence of impurity scatterings. The same feature can be seen in $\check{\Sigma}_{f_3}$ in Eq. (64), which implies the robustness of Δ_3. On the other hand, $\check{\Sigma}_{f_2}$ and $\check{\Sigma}_{f_4}$ have different matrix structures from their pair potentials shown in Table. I. In other words, the impurity self-energy leaves the pair potentials as they are. The previous studies suggested that the superconductivity in such cases can be fragile. We also note that $\check{\Sigma}_{f_2}$ and $\check{\Sigma}_{f_4}$ enhance the pair correlation belonging to odd-frequency spin-triplet even-momentum-parity even-orbital-parity symmetry. In what follows, we discuss the characteristic behavior of T_c as a function of impurity concentration case by case.

1. Δ_1

The gap equation for Δ_1 results in

$$\Delta_1 = g_1 T \sum_{\omega_n} \frac{1}{N} \sum_{\boldsymbol{k}} \frac{\tilde{\Delta}_1}{\tilde{Z}} \left[\tilde{\omega}_n^2 + \tilde{c}_{\boldsymbol{k}}^2 + m_{\boldsymbol{k}}^2 + V_x^2 + V_y^2 + V_z^2\right]. \tag{68}$$

By comparing with the gap equation in the clean limit in Eq. (34), the renormalized values are defined as

$$\tilde{\Delta}_1 = \Delta_1 (1 + \eta_n), \tag{69}$$

$$\tilde{Z}(\boldsymbol{k}, i\omega_n) = Z(\boldsymbol{k}, i\tilde{\omega}_n)|_{\mu \to \tilde{\mu}}, \tag{70}$$

$$\tilde{c}_{\boldsymbol{k}} = c_{\boldsymbol{k}}|_{\mu \to \tilde{\mu}}. \tag{71}$$

The impurity self-energy renormalizes the pair potential and the Matsubara frequency in the same manner as $\Delta_1 \to \tilde{\Delta}_1$ and $\omega_n \to \tilde{\omega}_n$ [1]. We solve the gap equation numerically and plot the transition temperature T_c of Δ_1 as a function of ξ_0/ℓ in Fig. 3. Here T_0 is the transition temperature in the clean limit, $\xi_0 = v_F/(2\pi T_0)$ is the superconducting coherence length, v_F is the Fermi velocity, $\ell = v_F \tau_{\rm imp}$ is the mean-free path due to impurity scatterings, and $\tau_{\rm imp}$ is the lifetime of a quasiparticle. We found that the normal part of self-energy $\check{\Sigma}_g$ is nearly independent of the Matsubara frequency in the low-energy region for $\omega_n \leqslant \omega_c$. Here $\omega_c = 10^3 T_0$ is the cutoff energy of the Matsubara frequency. Therefore, we estimate $\tau_{\rm imp}$ from the imaginary part of $\check{\Sigma}_g$ as

$$\frac{1}{\tau_{\rm imp}} = -2{\rm Tr}\left[\frac{1}{4}\,{\rm Im}\,\check{\Sigma}_g\right] \sim 2\pi \times n_{\rm imp} v_{\rm imp}^2 \times 10^{-2}\,[{\rm eV}]. \tag{72}$$

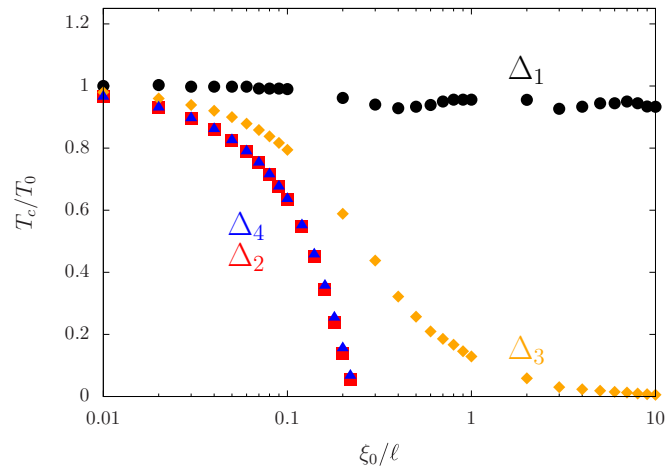

FIG. 3. The superconducting transition temperature T_c is plotted as a function of ξ_0/ℓ. The vertical axis is normalized to the transition temperature in the clean limit T_0. We fix T_0 for all pair potentials.

The horizontal axis ξ_0/ℓ in Fig. 3 is proportional to the impurity concentration $n_{\rm imp}$. The results in Fig. 3 show that T_c of Δ_1 is almost independent of the impurity concentration as shown with filled circles. Such behavior agrees well with T_c in a limiting case of idealistic models. The previous papers [6–9] considered two-band superconductivity with the intraband pairing order parameters (say D_1 and D_2) on idealistic two-band electronic structures and demonstrated that T_c is independent of impurity concentration at $D_1 = D_2$. The interband impurity scatterings disappear in such a symmetric situation, which explains the unchanged T_c. The superconducting state in Cu-doped Bi_2Se_3 with Δ_1 corresponds to the symmetric intraband pairing state in the previous studies. In this paper, we confirmed that the conclusions of the previous papers on idealistic band structures are valid even if we calculate T_c on a realistic electronic structure. In Fig. 3, the results for Δ_1 show the oscillating behavior. Although it is not easy to specify the reasons for the oscillations, such behavior comes from a realistic band structure. In the Born approximation, we conclude that T_c of Δ_1 is insensitive to the impurity scatterings.

2. Δ_3

The gap equation for Δ_3 becomes

$$\Delta_3 = g_3 T \sum_{\omega_n} \frac{1}{N} \sum_{\boldsymbol{k}} \frac{\Delta'_3}{\tilde{Z}} \left[\tilde{\omega}_n^2 + \tilde{c}_{\boldsymbol{k}}^2 - m_{\boldsymbol{k}}^2 + V_x^2 + V_y^2 - V_z^2\right], \tag{73}$$

$$\Delta'_3 = \Delta_3 (1 + \eta'_n). \tag{74}$$

The pair potential is renormalized by the impurity self-energy as $\Delta_3 \to \Delta'_3$ in Eq. (73) in a slightly different way from the relation $\omega_n \to \tilde{\omega}_n$. By solving Eq. (73), we plot T_c of Δ_3 as a function of ξ_0/ℓ in Fig. 3. The results show that T_c of the spin-singlet interorbital pairing order is suppressed slowly with the increase of ξ_0/ℓ and goes to zero in the dirty limit. A previous paper [10], however, demonstrated on an idealistic two-band structure that T_c of a spin-singlet

s-wave interband pairing order is independent of the impurity concentration. Thus Δ_3 in a Cu-doped Bi_2Se_3 is more fragile than that in an idealistic two-band model. The difference between the results in the two models can be explained by the enhancement of odd-frequency pairing components due to the realistic electronic structures. The odd-frequency pairing correlation is absent in an idealistic band structure [10]. As a result, the impurity self-energy renormalizes the pair potential and the Matsubara frequency in the same manner, which leads to unchanged T_c versus ξ_0/ℓ. In Cu-doped Bi_2Se_3, on the other hand, the asymmetry between two-orbitals ($m_{\boldsymbol{k}}$) and the orbital hybridization (V_z) generate the odd-frequency pairing correlations as described in Eq. (32). These correlations contribute negatively to the numerator of the renormalization factor of the pair potential $1+\eta'_n$ as shown in $-m_{\boldsymbol{k}}^2$ and $-V_z^2$ in Eq. (66). As a consequence, the reduction of the pair potential by odd-frequency pairs causes the suppression of T_c in the dirty regime. We conclude that the robustness of the spin-singlet s-wave interorbital pairing order depends on band structures.

3. Δ_2 and Δ_4

The gap equations for Δ_2 and Δ_4 result in

$$\Delta_2 = g_2 T \sum_{\omega_n} \frac{1}{N} \sum_{\boldsymbol{k}} \frac{\Delta_2}{\tilde{Z}} \big[\tilde{\omega}_n^2 + \tilde{c}_{\boldsymbol{k}}^2 - m_{\boldsymbol{k}}^2 + V_x^2 + V_y^2 + V_z^2 - 2J_n\omega_n\tilde{\omega}_n m_{\boldsymbol{k}}\big], \tag{75}$$

$$\Delta_4 = g_4 T \sum_{\omega_n} \frac{1}{N} \sum_{\boldsymbol{k}} \frac{\Delta_4}{\tilde{Z}} \big[\tilde{\omega}_n^2 + \tilde{c}_{\boldsymbol{k}}^2 - m_{\boldsymbol{k}}^2 + V_x^2 - V_y^2 + V_z^2 - 2J_n\omega_n\tilde{\omega}_n m_{\boldsymbol{k}}\big]. \tag{76}$$

Both Δ_2 and Δ_4 represent spin-triplet interorbital pairing order antisymmetric under the permutation of two orbitals. The numerical results in Fig. 3 indicate that T_c of Δ_2 and that of Δ_4 decrease rapidly with the increase of ξ_0/ℓ and vanish around $\xi_0/\ell \approx 0.3$. The impurity self-energy renormalizes the Matsubara frequency as $\omega_n \to \tilde{\omega}_n$. However, it leaves the pair potentials unchanged as shown in Eqs. (75) and (76). Therefore, Δ_2 and Δ_4 are fragile in the presence of impurities. The obtained results of T_c for a Cu-doped Bi_2Se_3 agree even quantitatively with those calculated in an idealistic band structure [10]. The interorbital impurity scatterings mix the electronic states in the two orbitals and average the pair potentials over the two orbital degree of freedom. As a result, the impurity scatterings wash out the sign of the pair potential in Eq. (17), which leads to the suppression of odd-orbital symmetric superconductivity. We confirmed that this physical interpretation is valid independent of band structures.

Several experiments have indicated nematic superconductivity in Cu-doped Bi_2Se_3 [27–29]. Such superconductivity can be realized when the pair potential belongs to the E_u representation of the D_{3d} point group [30]. The corresponding pair potential is described as

$$\check{\Delta}_{\text{nematic}} = \Delta(A_x\hat{s}_3(i\hat{\sigma}_2) + A_y\hat{s}_0(i\hat{\sigma}_2)), \tag{77}$$

where coefficients $A_{x,y}$ determine a nematic direction. Δ_4 corresponds to the specific case $[(A_x, A_y) = (1, 0)]$ of the nematic superconductivity. The nematic is considered to be fragile in the presence of potential disorder because the nematic order belongs to odd-orbital symmetry as well as Δ_2 and Δ_4.

Finally, we compare our results in the present paper with those in a recent study [31]. The authors of Ref. [31] formulated the random impurity scatterings based on the two-band picture in momentum space, which is obtained by diagonalizing the normal state Hamiltonian in the absence of impurities [32]. They mapped a Hamiltonian for an interorbital s-wave superconductor with random impurities to a Hamiltonian for a single-band unconventional superconductor with random impurities. As a result, they concluded that Δ_2, Δ_3, and Δ_4 are fragile under the potential disorder. Their conclusion for Δ_3 does not agree with ours obtained by applying the standard method [1]. The difference in the theoretical methods causes the discrepancy. An earlier [33] and a recent [34] analysis also contradict our results. A key point might be the self-energy due to interorbital impurity scatterings. Actually, all of the previous papers [6–10] suggested an importance of the interorbital/interband impurity scatterings on T_c. References [31,33,34], on the other hand, do not consider the interorbital impurity scatterings.

IV. CONCLUSION

We studied the effects of random nonmagnetic impurities on the superconducting transition temperature T_c in Cu-doped Bi_2Se_3. We consider four types of momentum-independent pair potentials, which include the intraorbital pairing (Δ_1), the interorbital-even-parity pairing (Δ_3), and the interorbital-odd-parity pairings (Δ_2 and Δ_4). The effects of the impurity scatterings are considered through the self-energy of the Green's function within the Born approximation. T_c of Δ_1 is insensitive to the impurity concentration, which is consistent with previous theories. We find that Δ_1 with the electronic structure of a Cu-doped Bi_2Se_3 corresponds to a limiting case of idealistic models [6–9]. T_c of Δ_3 decreases moderately with the increase of impurity concentration and vanishes in the dirty limit, which does not agree well with the results on an idealistic model [10]. The presence of the odd-frequency pairing correlations explain the discrepancy. T_c of Δ_2 and Δ_4 decrease rapidly with the increase of the impurity concentration. Superconductivity vanishes at a critical value of the impurity concentration. The results are consistent with those in an idealistic model even quantitatively [10].

We found that the robustness of the even-orbital-parity order parameters depends on the details of the band structures and that the odd-orbital-parity order parameters are fragile irrespective of the band structures.

ACKNOWLEDGMENTS

The authors are grateful to P. M. R. Brydon, D. C. Cavanagh, and K. Yada for useful discussions. This work was supported by JSPS KAKENHI (No. JP20H01857), JSPS Core-to-Core Program (A. Advanced Research Networks), and JSPS and Russian Foundation for Basic Research under Japan-Russia Research Cooperative Program Grant No. 19-52-50026.

APPENDIX A: RESTRICTION OF HOPPING MATRIX IN TIGHT-BINDING HAMILTONIAN

The crystal structure of Bi_2Se_3 preserves discrete symmetries [19,20] such as threefold rotation R_3 along the z direction, twofold rotation R_2 along the x direction, and inversion P. In addition, both the normal and superconducting states preserve time-reversal T symmetry. With the basis of $(|+,\uparrow\rangle, |-,\uparrow\rangle, |+,\downarrow\rangle, |-,\downarrow\rangle)$, these symmetry operations can be represented as $\check{R}_3 = \exp(i\frac{\pi}{3}\hat{s}_3\hat{\sigma}_0)$, $\check{R}_2 = i\hat{s}_1\hat{\sigma}_3$, $\check{P} = \hat{s}_0\hat{\sigma}_3$, and $\check{T} = i\hat{s}_2\hat{\sigma}_0\mathcal{K}$, respectively. Here $\mathcal{K}$ represents the complex conjugation.

Under threefold rotation symmetry, the relation

$$\langle \boldsymbol{R}, \sigma, s| H |\boldsymbol{R}+\boldsymbol{a}_i, \sigma', s'\rangle = \exp\left(i\frac{\pi}{3}(s_3' - s_3)\right) \langle \boldsymbol{R}, \sigma, s| H |\boldsymbol{R}+\boldsymbol{a}_j, \sigma', s'\rangle\,, \tag{A1}$$

is satisfied for $(\boldsymbol{a}_i, \boldsymbol{a}_j) = (\boldsymbol{a}_1, -\boldsymbol{a}_2)$, $(\boldsymbol{a}_2, -\boldsymbol{a}_3)$, and $(\boldsymbol{a}_3, \boldsymbol{a}_1)$. Under twofold rotation symmetry, the relation

$$\langle \boldsymbol{R}, \sigma, s| H |\boldsymbol{R}+\boldsymbol{a}_i, \sigma', s'\rangle = \sigma_3'\sigma_3 \langle \boldsymbol{R}, \sigma, \bar{s}| H |\boldsymbol{R}+\boldsymbol{a}_j, \sigma', \overline{s'}\rangle \tag{A2}$$

holds true for $(\boldsymbol{a}_i, \boldsymbol{a}_j) = (\boldsymbol{a}_1, -\boldsymbol{a}_3)$, $(\boldsymbol{a}_2, -\boldsymbol{a}_2)$, and $(\boldsymbol{a}_3, -\boldsymbol{a}_1)$. As a result of inversion symmetry, we find the relation of

$$\langle \boldsymbol{R}, \sigma, s| H |\boldsymbol{R}+\boldsymbol{a}_i, \sigma', s'\rangle = \sigma_3'\sigma_3 \langle \boldsymbol{R}, \sigma, s| H |\boldsymbol{R}-\boldsymbol{a}_i, \sigma', s'\rangle\,. \tag{A3}$$

Finally, time-reversal symmetry is described as

$$\langle \boldsymbol{R}, \sigma, s| H |\boldsymbol{R}+\boldsymbol{a}_i, \sigma', s'\rangle = s_3' s_3 \langle \boldsymbol{R}, \sigma', \overline{s'}| H |\boldsymbol{R}-\boldsymbol{a}_i, \sigma, \bar{s}\rangle\,. \tag{A4}$$

We have used the notation of

$$\sigma_3 = \begin{cases} +1 & (\sigma = +) \\ -1 & (\sigma = -), \end{cases} \quad s_3 = \begin{cases} +1 & (s = \uparrow) \\ -1 & (s = \downarrow), \end{cases} \tag{A5}$$

$$\overline{\sigma} = \begin{cases} - & (\sigma = +) \\ + & (\sigma = -), \end{cases} \quad \bar{s} = \begin{cases} \downarrow & (s = \uparrow) \\ \uparrow & (s = \downarrow). \end{cases} \tag{A6}$$

According to the conditions in Eqs. (A1)–(A4), the hopping matrices can be reduced as [21,23]

$$\check{t}_{\boldsymbol{a}_1} = \begin{pmatrix} t_{11} & t_{12} & 0 & t_{14} \\ -t_{12} & t_{22} & t_{14} & 0 \\ 0 & -t_{14}^* & t_{11} & t_{12} \\ -t_{14}^* & 0 & -t_{12} & t_{22} \end{pmatrix}, \quad \check{t}_{-\boldsymbol{a}_1} = \begin{pmatrix} t_{11} & -t_{12} & 0 & -t_{14} \\ t_{12} & t_{22} & -t_{14} & 0 \\ 0 & t_{14}^* & t_{11} & -t_{12} \\ t_{14}^* & 0 & t_{12} & t_{22} \end{pmatrix}, \tag{A7}$$

$$\check{t}_{\boldsymbol{a}_2} = \begin{pmatrix} t_{11} & -t_{12} & 0 & -e^{i2\pi/3}t_{14} \\ t_{12} & t_{22} & -e^{i2\pi/3}t_{14} & 0 \\ 0 & -e^{i2\pi/3}t_{14} & t_{11} & -t_{12} \\ -e^{i2\pi/3}t_{14} & 0 & t_{12} & t_{22} \end{pmatrix}, \quad \check{t}_{-\boldsymbol{a}_2} = \begin{pmatrix} t_{11} & t_{12} & 0 & e^{i2\pi/3}t_{14} \\ -t_{12} & t_{22} & e^{i2\pi/3}t_{14} & 0 \\ 0 & e^{i2\pi/3}t_{14} & t_{11} & t_{12} \\ e^{i2\pi/3}t_{14} & 0 & -t_{12} & t_{22} \end{pmatrix}, \tag{A8}$$

$$\check{t}_{\boldsymbol{a}_3} = \begin{pmatrix} t_{11} & t_{12} & 0 & -t_{14}^* \\ -t_{12} & t_{22} & -t_{14}^* & 0 \\ 0 & t_{14} & t_{11} & t_{12} \\ t_{14} & 0 & -t_{12} & t_{22} \end{pmatrix}, \quad \check{t}_{-\boldsymbol{a}_3} = \begin{pmatrix} t_{11} & -t_{12} & 0 & t_{14}^* \\ t_{12} & t_{22} & t_{14}^* & 0 \\ 0 & -t_{14} & t_{11} & -t_{12} \\ -t_{14} & 0 & t_{12} & t_{22} \end{pmatrix}, \tag{A9}$$

$$\check{t}_{\boldsymbol{a}_4} = \begin{pmatrix} t_{11}' & t_{12}' & 0 & 0 \\ -t_{12}' & t_{22}' & 0 & 0 \\ 0 & 0 & t_{11}' & t_{12}' \\ 0 & 0 & -t_{12}' & t_{22}' \end{pmatrix}, \quad \check{t}_{-\boldsymbol{a}_4} = \begin{pmatrix} t_{11}' & -t_{12}' & 0 & 0 \\ t_{12}' & t_{22}' & 0 & 0 \\ 0 & 0 & t_{11}' & -t_{12}' \\ 0 & 0 & t_{12}' & t_{22}' \end{pmatrix}. \tag{A10}$$

In momentum space, the tight-binding Hamiltonian becomes

$$\check{H}_N(\boldsymbol{k}) = \begin{pmatrix} c_{\boldsymbol{k}} + m_{\boldsymbol{k}} & -i(v_3\alpha_3(\boldsymbol{k}) + v_z\alpha_z(\boldsymbol{k})) & 0 & v(\alpha_y(\boldsymbol{k}) + i\alpha_x(\boldsymbol{k})) \\ i(v_3\alpha_3(\boldsymbol{k}) + v_z\alpha_z(\boldsymbol{k})) & c_{\boldsymbol{k}} - m_{\boldsymbol{k}} & v(\alpha_y(\boldsymbol{k}) + i\alpha_x(\boldsymbol{k})) & 0 \\ 0 & v(\alpha_y(\boldsymbol{k}) - i\alpha_x(\boldsymbol{k})) & c_{\boldsymbol{k}} + m_{\boldsymbol{k}} & -i(v_3\alpha_3(\boldsymbol{k}) + v_z\alpha_z(\boldsymbol{k})) \\ v(\alpha_y(\boldsymbol{k}) - i\alpha_x(\boldsymbol{k})) & 0 & i(v_3\alpha_3(\boldsymbol{k}) + v_z\alpha_z(\boldsymbol{k})) & c_{\boldsymbol{k}} - m_{\boldsymbol{k}} \end{pmatrix}, \tag{A11}$$

with

$$c_{\boldsymbol{k}} = -\mu + c_1\alpha_1(\boldsymbol{k}) + c_2\alpha_2(\boldsymbol{k}), \quad m_{\boldsymbol{k}} = m_0 + m_1\alpha_1(\boldsymbol{k}) + m_2\alpha_2(\boldsymbol{k}), \tag{A12}$$

$$c_1 = -\frac{c^2}{2}(t'_{11} + t'_{22}), \quad c_2 = -\frac{3a^2}{4}(t_{11} + t_{22}), \quad \mu = -3(t_{11} + t_{22}) - (t'_{11} + t'_{22}) - \varepsilon, \tag{A13}$$

$$m_1 = -\frac{c^2}{2}(t'_{11} - t'_{22}), \quad m_2 = -\frac{3a^2}{4}(t_{11} - t_{22}), \quad m_0 = 3(t_{11} - t_{22}) + t'_{11} - t'_{22}, \tag{A14}$$

$$v = -3ie^{i2\pi/3}at_{14}, \quad v_z = -2ct'_{12}, \quad v_3 = \frac{3a^3}{4}t_{12}. \tag{A15}$$

Here $\alpha_1(\boldsymbol{k})$, $\alpha_2(\boldsymbol{k})$, $\alpha_x(\boldsymbol{k})$, $\alpha_y(\boldsymbol{k})$, and $\alpha_z(\boldsymbol{k})$, are defined in Eqs. (10)–(14). We also define $\alpha_3(\boldsymbol{k}) = -\frac{8}{3a^3}(2\cos\frac{\sqrt{3}}{2}k_x a \sin\frac{1}{2}k_y a - \sin k_y a)$. In this paper, we set the parameters as follows [21,35]: $a = 4.14$ Å, $c = 28.7$ Å, $\mu = 0.5$ eV, $c_2 = 30.4$ eVÅ^2, $m_0 = -0.28$ eV, $m_2 = 44.5$ eVÅ^2, $v = 3.33$ eVÅ, $c_1/c^2 = 0.024$ eV, $m_1/c^2 = 0.20$ eV, and $v_z/c = 0.32$ eV. We choose $v_3 = 0$ for simplicity [19,20].

APPENDIX B: UNITARY EQUIVALENCE OF THE HAMILTONIAN WITH INTRAORBITAL PAIRING ORDER

The superconducting state with s-wave spin-singlet intraorbital pairing order is described by the following Bogoliubov-de Gennes Hamiltonian [9]:

$$\bar{H}^{(0)}_{\boldsymbol{k}}(\theta, \varphi_1, \varphi_2) = \begin{bmatrix} \xi_1 & -iV_z e^{i\theta} & 0 & Ve^{i\theta} & 0 & 0 & \Delta_+ & 0 \\ iV_z e^{-i\theta} & \xi_2 & Ve^{-i\theta} & 0 & 0 & 0 & 0 & \Delta_- \\ 0 & V^* e^{i\theta} & \xi_1 & -iV_z e^{i\theta} & -\Delta_+ & 0 & 0 & 0 \\ V^* e^{-i\theta} & 0 & iV_z e^{-i\theta} & \xi_2 & 0 & -\Delta_- & 0 & 0 \\ 0 & 0 & -\Delta_+^* & 0 & -\xi_1 & iV_z e^{-i\theta} & 0 & V^* e^{-i\theta} \\ 0 & 0 & 0 & -\Delta_-^* & -iV_z e^{i\theta} & -\xi_2 & V^* e^{i\theta} & 0 \\ \Delta_+^* & 0 & 0 & 0 & 0 & Ve^{-i\theta} & -\xi_1 & iV_z e^{-i\theta} \\ 0 & \Delta_-^* & 0 & 0 & Ve^{i\theta} & 0 & -iV_z e^{i\theta} & -\xi_2 \end{bmatrix}, \tag{B1}$$

$$\xi_1 = c_{\boldsymbol{k}} + m_{\boldsymbol{k}}, \quad \xi_2 = c_{\boldsymbol{k}} - m_{\boldsymbol{k}}, \quad V = v(\alpha_y(\boldsymbol{k}) + i\alpha_x(\boldsymbol{k})), \quad V_z = v_z\alpha_z(\boldsymbol{k}), \tag{B2}$$

$$\Delta_+ = \frac{g_+}{N}\sum_{\boldsymbol{k}}\langle\psi_{+,\uparrow}(\boldsymbol{k})\psi_{+,\downarrow}(-\boldsymbol{k})\rangle = |\Delta_+|e^{i\varphi_1}, \tag{B3}$$

$$\Delta_- = \frac{g_-}{N}\sum_{\boldsymbol{k}}\langle\psi_{-,\uparrow}(\boldsymbol{k})\psi_{-,\downarrow}(-\boldsymbol{k})\rangle = |\Delta_-|e^{i\varphi_2}, \tag{B4}$$

where $g_\sigma > 0$ represents the attractive interaction between two electrons in the orbital σ and θ denotes the phase of the hybridization in the normal state. We obtain the normal part of $\bar{H}^{(0)}_{\boldsymbol{k}}(\theta, \varphi_1, \varphi_2)$ from Eq. (5) by choosing $\psi_{+,s} \to \psi_{+,s}e^{i\theta/2}$ and $\psi_{-,s} \to \psi_{-,s}e^{-i\theta/2}$. Although the phase factor $e^{i\theta}$ does not affect the physics in the normal state, such a gauge transformation affects the relative phase difference between the order parameters $\varphi_1 - \varphi_2$ [9].

Time-reversal symmetry of $\bar{H}^{(0)}_{\boldsymbol{k}}$ is represented by

$$\bar{\mathcal{T}}\bar{H}^{(0)}_{\boldsymbol{k}}\bar{\mathcal{T}}^{-1} = \bar{H}^{(0)}_{-\boldsymbol{k}}, \quad \bar{\mathcal{T}} = \hat{\tau}_0(i\hat{s}_2)\hat{\sigma}_0\mathcal{K}. \tag{B5}$$

If we find a transformation $\bar{U}$ which eliminates all the phase factors in Eq. (B1), it is possible to show time-reversal symmetry of $\bar{H}^{(0)}_{\boldsymbol{k}}$ [9]. By applying the unitary transformation,

$$\bar{U} = \mathrm{diag}[e^{-i\varphi_1/2}, e^{-i\varphi_2/2}, e^{-i\varphi_1/2}, e^{-i\varphi_2/2}, e^{i\varphi_1/2}, e^{i\varphi_2/2}, e^{i\varphi_1/2}, e^{i\varphi_2/2}], \tag{B6}$$

the Hamiltonian is transformed into

$$\bar{U}\bar{H}^{(0)}_{\boldsymbol{k}}(\theta, \varphi_1, \varphi_2)\bar{U}^\dagger = \bar{H}^{(0)}_{\boldsymbol{k}}\left(\theta - \frac{\varphi_1 - \varphi_2}{2}, 0, 0\right). \tag{B7}$$

Therefore, the three phases must satisfy a relation

$$2\theta - \varphi_1 + \varphi_2 = 2\pi n, \tag{B8}$$

with n being an integer for the Hamiltonian to preserve time-reversal symmetry. By tuning $\theta = 0$ at $n = 0$, the two pair potentials have the same sign as each other because of $\varphi_1 - \varphi_2 = 0$. By tuning $\theta = \pi/2$, on the other hand, $\bar{H}^{(0)}_{\boldsymbol{k}}(\pi/2, 0, \pi)$ describes a state where two pair potentials have the opposite sign as each other. It is easy to show that $\bar{H}^{(0)}_{\boldsymbol{k}}(\pi/2, 0, \pi)$ and $\bar{H}^{(0)}_{\boldsymbol{k}}(0, 0, 0)$ are unitary equivalent to each other. We set $g_+ = g_- = g_1$ and $\Delta_+ = \Delta_- = \Delta_1$ in Sec. II. Under the condition, $\Delta_1(i\hat{s}_2)\hat{\sigma}_3$ is unitary equivalent to $\breve{\Delta}_1 = \Delta_1(i\hat{s}_2)\hat{\sigma}_0$.

[1] A. A. Abrikosov, L. P. Gor'kov, and I. E. Dzyaloshinski, *Methods of Quantum Field Theory in Statistical Physics* (Dover Publications, New York, 1975).

[2] A. A. Abrikosov and L. P. Gor'kov, Zh. Eksp. Teor. Fiz. **36**, 319 (1959) [Sov. Phys. JETP **9**, 220 (1959)].

[3] P. Anderson, J. Phys. Chem. Solids **11**, 26 (1959).

[4] Y. Sun and K. Maki, Phys. Rev. B **51**, 6059 (1995).

[5] P. B. Allen and B. Mitrovic, *Theory of Superconducting T_c* (Academic Press, New York, 1983), Vol. 37, pp. 1–92.

[6] A. A. Golubov and I. I. Mazin, Phys. Rev. B **55**, 15146 (1997).

[7] D. V. Efremov, M. M. Korshunov, O. V. Dolgov, A. A. Golubov, and P. J. Hirschfeld, Phys. Rev. B **84**, 180512(R) (2011).

[8] M. M. Korshunov, Y. N. Togushova, and O. V. Dolgov, Phys. Usp. **59**, 1211 (2016).

[9] Y. Asano and A. A. Golubov, Phys. Rev. B **97**, 214508 (2018).

[10] Y. Asano, A. Sasaki, and A. A. Golubov, New J. Phys. **20**, 043020 (2018).

[11] Y. Kamihara, T. Watanabe, M. Hirano, and H. Hosono, J. Am. Chem. Soc. **130**, 3296 (2008).

[12] K. Kuroki, S. Onari, R. Arita, H. Usui, Y. Tanaka, H. Kontani, and H. Aoki, Phys. Rev. Lett. **101**, 087004 (2008).

[13] J. Nagamatsu, N. Nakagawa, T. Muranaka, Y. Zenitani, and J. Akimitsu, Nature **410**, 63 (2001).

[14] H. J. Choi, D. Roundy, H. Sun, M. L. Cohen, and S. G. Louie, Nature **418**, 758 (2002).

[15] Y. S. Hor, A. J. Williams, J. G. Checkelsky, P. Roushan, J. Seo, Q. Xu, H. W. Zandbergen, A. Yazdani, N. P. Ong, and R. J. Cava, Phys. Rev. Lett. **104**, 057001 (2010).

[16] L. Fu and E. Berg, Phys. Rev. Lett. **105**, 097001 (2010).

[17] S. Onari and H. Kontani, Phys. Rev. Lett. **103**, 177001 (2009).

[18] S. Sasaki, M. Kriener, K. Segawa, K. Yada, Y. Tanaka, M. Sato, and Y. Ando, Phys. Rev. Lett. **107**, 217001 (2011).

[19] H. Zhang, C.-X. Liu, X.-L. Qi, X. Dai, Z. Fang, and S.-C. Zhang, Nat. Phys. **5**, 438 (2009).

[20] C.-X. Liu, X.-L. Qi, H. J. Zhang, X. Dai, Z. Fang, and S.-C. Zhang, Phys. Rev. B **82**, 045122 (2010).

[21] T. Hashimoto, K. Yada, A. Yamakage, M. Sato, and Y. Tanaka, J. Phys. Soc. Jpn. **82**, 044704 (2013).

[22] L. A. Wray, S.-Y. Xu, Y. Xia, Y. S. Hor, D. Qian, A. V. Fedorov, H. Lin, A. Bansil, R. J. Cava, and M. Z. Hasan, Nat. Phys. **6**, 855 (2010).

[23] S. Mao, A. Yamakage, and Y. Kuramoto, Phys. Rev. B **84**, 115413 (2011).

[24] A. J. Leggett, Prog. Theor. Phys. **36**, 901 (1966).

[25] A. M. Black-Schaffer and A. V. Balatsky, Phys. Rev. B **88**, 104514 (2013).

[26] Y. Asano and A. Sasaki, Phys. Rev. B **92**, 224508 (2015).

[27] K. Matano, M. Kriener, K. Segawa, Y. Ando, and G.-q. Zheng, Nat. Phys. **12**, 852 (2016).

[28] S. Yonezawa, K. Tajiri, S. Nakata, Y. Nagai, Z. Wang, K. Segawa, Y. Ando, and Y. Maeno, Nat. Phys. **13**, 123 (2017).

[29] R. Tao, Y.-J. Yan, X. Liu, Z.-W. Wang, Y. Ando, Q.-H. Wang, T. Zhang, and D.-L. Feng, Phys. Rev. X **8**, 041024 (2018).

[30] L. Fu, Phys. Rev. B **90**, 100509(R) (2014).

[31] D. C. Cavanagh and P. M. R. Brydon, Phys. Rev. B **101**, 054509 (2020).

[32] K. Michaeli and L. Fu, Phys. Rev. Lett. **109**, 187003 (2012).

[33] Y. Nagai, Phys. Rev. B **91**, 060502(R) (2015).

[34] L. Andersen, A. Ramires, Z. Wang, T. Lorenz, and Y. Ando, Sci. Adv. **6**, eaay6502 (2020).

[35] T. Mizushima, A. Yamakage, M. Sato, and Y. Tanaka, Phys. Rev. B **90**, 184516 (2014).